

# Miniaturized Microstrip AIA by means of Metamaterial substrate with application in Wireless Identifications and wireless Sensors

Mehdi KarimiMeh, Ali Agharasouli, Amin Darvazehban

**Abstract**— Miniaturized integrated active microstrip patch antenna which operates at 930 MHz is investigated theoretically and experimentally. The rectangular patch antenna is loaded by Embedded Split Ring Resonators (ESRR) to modify the substrate constitutive parameters. As a result, the engineered substrate works as magneto-dielectric substrate which miniaturize the antenna patch up to 70 % compared to a regular non-loaded substrate antenna. The miniaturized antenna is then integrated with a transistor based oscillator. The proposed low profile self-oscillating antenna can be used as a RF beacon or wireless wave generator for wireless power transmission applications.

**Index Terms**— Embedded split ring resonators, miniaturized microstrip antenna, self-oscillating antenna, wireless identification, wireless power transmission, Ga-As FET transistor

## 1 INTRODUCTION

LOW profile hand held wireless devices and low power consumption sensors have attracted a lot of attention in recent years. It leads that wireless power transmission and charging to become one of the most important part of next generation of mobile devices [1].

Low cost wireless sensors and wireless identification systems are among the inevitable part of Wireless Sensor Network (WSN). Active Integrated Antennas (AIAs) are a promising circuits to provide RF signals to be used in wireless systems when RF power is needed to enhance the wireless transceivers [2]-[7]. The applications of wireless tags and sensors are extensive, for example in [8] it is shown one application of RF tags for the crack detection in concrete structures which is easier compare to other methods [9]. The AIA is a self-oscillating antenna which is integrated by an oscillator to generate the RF signal in a desired frequency band. The antenna acts as the resonator of the oscillator and radiate the RF signal. AIAs can be placed in an array to form a retrodirective antenna in power spatial combining applications [10], [11]. The AIAs have found interests to wake up tags to increase the efficiency of the wireless communication.

There are several methods to miniaturize a microstrip patch antenna. Using metamaterial structure such as Split Ring Resonators (SRRs) or Complimentary SRRs (CSRRs) is a promising way to manipulate the constitutive parameters of the substrate in order to change its electromagnetic characteristics and wave propagation regime [12]-[18]. A stack of slabs with SRRs provides a magneto-dielectric substrate by manipulating its permeability constant [19], [20].

These loaded substrates need a minimum height to accommodate those slabs which leads to have a bulky structure. In [21], for the first time, an Embedded SRRs (ESRRs) were proposed to have ultra-thin magneto-dielectric substrate. This embedded resonator can be used to miniaturize substrate integrated waveguides [22], or to provide adjustable uniaxial medium to form tunable pass or stop bands in filter applications [23].

In order to reach a low profile and inexpensive active antenna systems, the antenna miniaturizing techniques have been investigated recently [24], [25]. The loaded SRRs with an external capacitor form the radiator and acts as a resonator in the antenna structure. These antennas provide omnidirectional radiation pattern which can be a positive aspect for some applications, however for the configurations where a tag must be attached on metallic or ground surface, directive antennas are more efficient. In [6] a CSRR loaded structure is used to miniaturize the AIA.

In this paper, we proposed a novel ESRRs configuration with interdigital capacitor to reduce the frequency resonance. The antenna consists of two layers, bottom and top substrate layers. The ESRRs are placed on the bottom substrate surface and the patch antenna is on the top layer. The dimensions of the ESRRs are optimized to have the maximum of constitutive parameters and minimum of the magnetic and electric loss tangents. It leads the patch antenna resonates at a lower frequency band compared with a patch with conventional substrate and the same size. Each substrate height is 0.762 mm with  $\epsilon_r=3$  and  $\mu_r = 1$ . The proposed magneto-dielectric substrate provides the product constitutive parameters equal to around 12. Thus the size of the antenna is reduced up to 70 % compare to non-loaded substrate. The antenna is connected to the Negative Resistance Oscillator

(NRO) circuit which is realized by using a Heterojunction GaAs FET transistor.

The antenna acts as a resonator circuit with specific input impedance. The active circuit produces RF power for the antenna (load) to propagate.

## 2 MINIATURIZED MICROSTRIP ANTENNA WITH MAGNETO-DIELECTRIC SUBSTRATE

The operation frequency of rectangular microstrip patch antenna can be obtained approximately by Eq. (1) which is shown in [26].

$$f_r = \frac{c}{2(L + h)\sqrt{\epsilon_{eff}\mu_{eff}}} \quad (1)$$

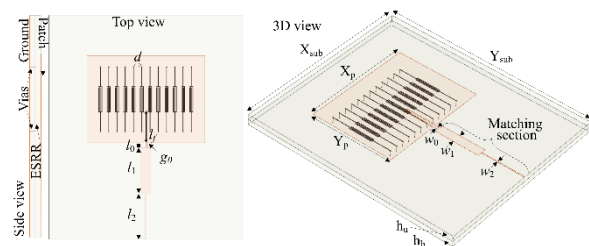


Figure 1: The patch antenna on the magneto-dielectric substrate.

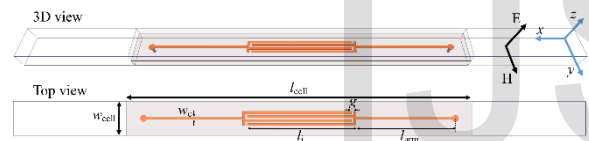


Figure 2: The dimensions of the ESRR unitcell.

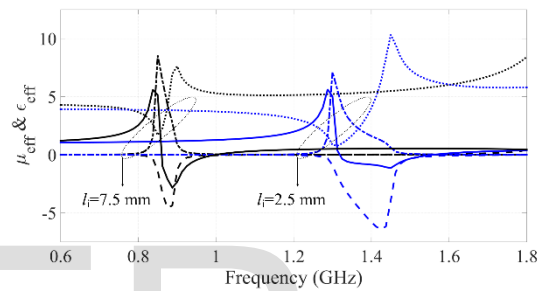
where  $c$  is the speed of light,  $L$  is the length of the patch,  $h$  is the substrate height,  $\epsilon_{eff}$  and  $\mu_{eff}$  are the substrate effective permittivity constant and permeability constant, respectively. The effective permeability constant of commercial substrate is one. Thus, by increasing the dielectric effective permittivity constant, the operation frequency is decreased with the same patch size which can be interpreted as miniaturizing the antenna. Using high permittivity substrate, increases the Q factor. This reduces the antenna radiation efficiency and increases the impedance at the edge of the patch which causes mismatch impedance at the antenna input port. In addition, the high permittivity substrate for microwave circuit is expensive. In [20], it is shown that a magneto-dielectric substrate with  $\mu_{eff} > 1$  improves the balance of magnetic and electric stored energy in the radiator. Thus, the operation bandwidth is maintained by miniaturizing the antenna with magneto-dielectric substrate.

Figure 1 shows the proposed magneto-dielectric substrate. The proposed ESRRs are placed on the bottom dielectric substrate surface. The patch antenna is placed on the top layer. The substrates are RO3203 with  $\epsilon_{eff} = 3$ ,  $h = 0.762$  mm. The ESRR consists of two vias connected to the ground in one

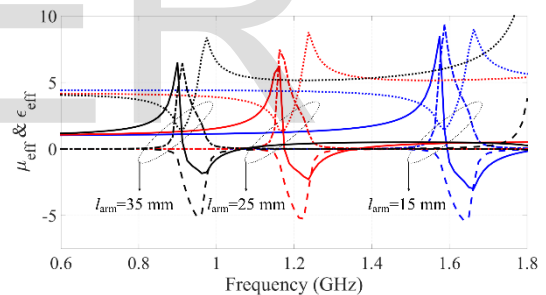
side and to the interdigital capacitor with two narrow strips on the other side. Thus, the embedded ESRR structure forms an embedded rectangular loop.

Magnetic fields normal to the surface of the ESRRs, induce currents which oscillates at the  $f_r$ . The induced current produces an equivalent magnetic dipole moment, which changes the effective magnetic permeability constant in the applied field direction [27]. Here, the patch antenna is placed on the top layer and its magnetic fields are perpendicular to the ESRRs surface in the dominate mode operation, see Fig.1. Thus, if the operation frequency of the patch antenna is designed close to the  $f_r$ , the effective constitutive parameters of the ESRR loaded substrate are changed.

The constitutive parameters of a periodic structure can be extracted by applying specific boundary condition to support Transvers Electric Magnetic (TEM) wave in Electromagnetics (EM) software [28]. The obtained results from this method are



(a)



(b)

Figure 3: The effective constitutive parameters for different (a)  $l_i$ , (b)  $l_{arm}$  values. The solid lines are  $\mu'(y)_{eff}$ , the dotted lines are  $\epsilon'(z)_{eff}$ , the dot-dashed lines are  $\mu''(y)_{eff}$  and the dashed lines are  $\epsilon''(z)_{eff}$ .

highly accurate even if the whole structure is not excited by a pure TEM wave, since the unitcell size is small compare to the operation wavelength [19, 21, 22]. The proposed ESRR unit cell is shown in Fig. 2.

The ESRRs dimensions determine the resonance frequency. The unitcell is simulated in HFSS to calculate its S-parameters. By using the S-parameter and the length of the unitcell  $l_{cell}$ , the effective dielectric permittivity and magnetic permeability are extracted by using the method introduced in [28]. Since, the permittivity and permeability constant are determined by electric and magnetic fields respectively, the extracted constitutive parameters are in the direction of each

field. Thus, the constitutive parameters in other direction can be assumed as same as the substrate parameters.

The constitutive parameters show a resonance behavior which is investigated for SRR structure in [27] as following:

$$\mu_{eff}^z = 1 - \frac{f_{mp}^2 - f_0^2}{f^2 - f_0^2 - j\gamma f} \quad (2)$$

Where,  $f_{mp}$  is the magnetic plasma frequency (in the lossless case,  $\mu_{eff}^z = 0$ ),  $f_0$  is the resonance frequency of the ESRR, and  $\gamma$  models losses. The equivalent magnetic dipole of ESSR is the reason of the effective dielectric permittivity variations. In [27] it is shown that when a parallel electric field illuminates a periodic array of metallic wires, the equivalent electrical dipole is generated. The ESRRs vias are parallel to the electric field and change the  $\epsilon_{eff}^z$  either. Thus there is also a variation in the dielectric permittivity constant.

The goal is that the magneto-dielectric substrate reaches to the maximum value of  $\mu_{eff}^z \times \epsilon_{eff}^z$  at  $f=930$  MHz with minimum losses to achieve the smallest patch size with the

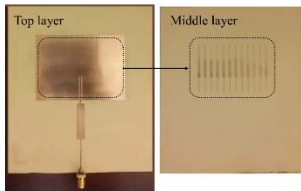


Figure 4: The miniaturized microstrip antenna, the embedded resonator is in the middle layer beneath the patch antenna.

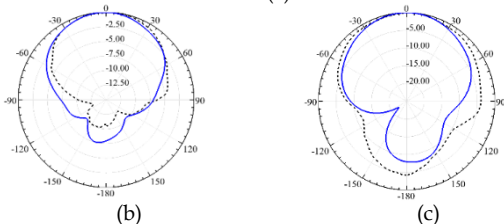
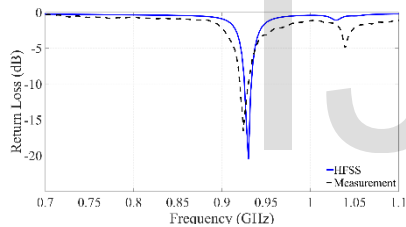


Fig. 5: (a) The return loss of the antenna, (b) the normalized radiation pattern in H-plane (c) and E-plane. The solid blue lines are simulation and short dashed black ones are measurement.

maximum radiation efficiency and bandwidth. There are several parameters to adjust the frequency response of the ESRRs. To investigate the frequency response of the proposed ESRR, the effective permittivity constant in the z direction  $\epsilon_{eff}^z$  and the effective permeability constant in the y direction  $\mu_{eff}^y$  is extracted from the simulated S-parameters of the unit cell for different dimensions.

The unitcell dimensions in mm are as following:  $l_{cell} = 33, w_{cell} = 3, l_i = 10, l_{arm} = 10, w_c = 2$  and  $r_{via} = 0.125$ . Figure

3 shows the  $\epsilon_{eff}^{\prime(z)}, \epsilon_{eff}^{\prime\prime(z)}, \mu_{eff}^{\prime(y)}$  and  $\mu_{eff}^{\prime\prime(y)}$  as the real and imaginary parts of the constitutive parameters for different values of  $l_i$  and  $l_{arm}$  while the other dimensions are fixed. As can be seen in Fig. 3(a) and Fig. 3(b), the resonance frequency of the ESSR increases by decreasing the length of the  $l_i$  or  $l_{arm}$ .

This is predictable since by shorting the length of  $l_i$  and  $l_{arm}$ , the associated inductor and capacitor decreases, respectively, results in  $f_0$  increase.

We are interested to work in region below resonance frequency of ESRR,  $f_0$ , since the electric and magnetic loss tangent  $\tan\delta_e = \frac{\epsilon_{eff}^{\prime\prime z}}{\epsilon_{eff}^{\prime z}}$ ,  $\tan\delta_m = \frac{\mu_{eff}^{\prime\prime y}}{\mu_{eff}^{\prime y}}$  are high at the resonance frequency, which reduce the radiation efficiency dramatically. It should be noticed that at  $f > f_0$  we have  $\mu_{eff}^z < 0$ , which leads to form a lossy media for wave propagation in the substrate. The antenna is optimized to resonate at 930 MHz by tuning the size of the ESRR around the highest value of the constitutive parameters. The inserted gap along

Table I

Parameter	Magneto-dielectric Substrate ( $\epsilon_{\mu}=12$ )	Rogers 3203 Substrate ( $\epsilon_{\mu}=3$ )	Parameters	Magneto-dielectric Substrate ( $\epsilon_{\mu}=12$ )	Rogers 3203 Substrate ( $\epsilon_{\mu}=3$ )
$X_{sub}$	105.6 mm	183 mm	$l_f$	17.4 mm	26 mm
$Y_{sub}$	125.6 mm	283.55 mm	$g_a$	0.6mm	0.25 mm
$X_p$	64.3 mm	116 mm	$h_a$	0.762 mm	0.762 mm
$Y_p$	47.35 mm	94 mm	$h_b$	0.762 mm	0.762 mm
$w_0$	1.2 mm	4 mm	$l_{arm}$	10.5 mm	-
$w_1$	5.3 mm	4 mm	$w_c$	0.3 mm	-
$w_2$	0.5 mm	4 mm	$l_i$	13.4 mm	-
$l_0$	2.6 mm	10 mm	$r_v$	0.125 mm	-
$l_1$	2.5 mm	25 mm	$g$	0.25 mm	-
$l_2$	24.7 mm	25 mm	$d$	4.5 mm	-

with the matching circuit are optimized to reach the minimized patch size with the best performance.

The proposed microstrip patch antenna with magneto-dielectric substrate is simulated and fabricated, see Fig. 4. The dimensions of the miniaturized patch antenna are  $Y_p = 47.35$  mm and  $X_p = 64.3$  mm to operate at 930 MHz. The dimensions of a patch antenna on the un-loaded substrate would be  $Y_p = 94$  mm and  $X_p = 116$  mm. Thus, the patch area of the miniaturized antenna is only 28 % of the conventional antenna at 930 MHz. In another word, by using Eq. (1), the value of  $\epsilon_{eff}^z \times \mu_{eff}^y = 11.5$  for the magneto-dielectric substrate which is around four times of the unloaded substrates. The  $S_{11}$  parameter and the antenna radiation pattern are measured and shown in Fig. 5. The dimensions of the miniaturized antenna compared with a conventional antenna are gathered in Table. I.

### 3 ACTIVE INTEGRATED ANTENNA

The antenna can be used as the resonator in the feedback loop to satisfy Barkhausencriterion [3, 6, 7, 24, 25] or connected to the active device with negative input impedance [4, 11,29].

In this paper, we integrated the proposed miniaturized antenna in UHF band with a negative resistance transistor based oscillator. The negative resistance circuits are used extensively in RF and microwave frequency oscillators [30].

The input impedance of the negative resistance circuit  $Z_{in}^{NRC}(w)$  is connected to the antenna input impedance  $Z_{in}^{Antenna}(w)$ , Fig. 6. From [29], the circuit oscillates at  $w_0$  if:

$$Z_{in}^{Antenna}(jw_0) + Z_{in}^{NRC}(jw_0) = 0 \quad (3)$$

If the sum of the real part of Eq. (3) is larger than zero ( $R_{in}^{Antenna}(j\omega_0) + R_{in}^{NRC}(j\omega_0) > 0$ ), the load power consumption is larger than the produced energy and oscillation will die out. In the other hand, if  $R_{in}^{Antenna}(j\omega_0) + R_{in}^{NRC}(j\omega_0) < 0$ , the circuit is unstable and the amplitude will be increased until the circuit is saturated.

The negative input impedance can be realized by Gunn diodes [4, 11], tunnel diodes [29] or transistors [2]. The DC power consumption of Gunn diode is high which is not good for low profile systems with limited power source. The tunnel diodes are almost discontinued from production and their input power is highly restricted due to their very low DC bias point [31]. Here, we used a Hetrojunction GaAs FET transistor in common source mode to generate the negative input impedance.

To design the active circuit in order to satisfy the oscillation condition, the transistor must be in potentially unstable region. In [30], the instability circles condition in order to maintain the input reflection coefficient ( $\Gamma_{in}$ ) and output reflection coefficient ( $\Gamma_{out}$ ) larger than one is investigated. The reflection coefficient larger

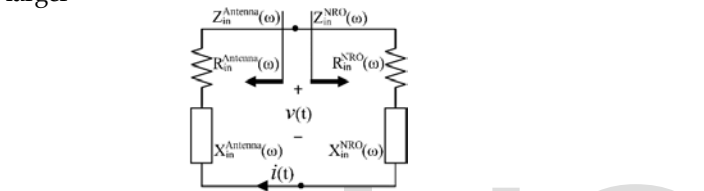


Figure 6: The circuit model of negative resistance oscillator which is connected to the antenna as a resonator and radiator.

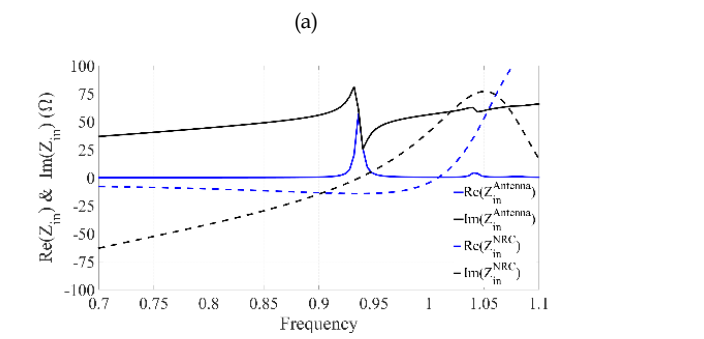
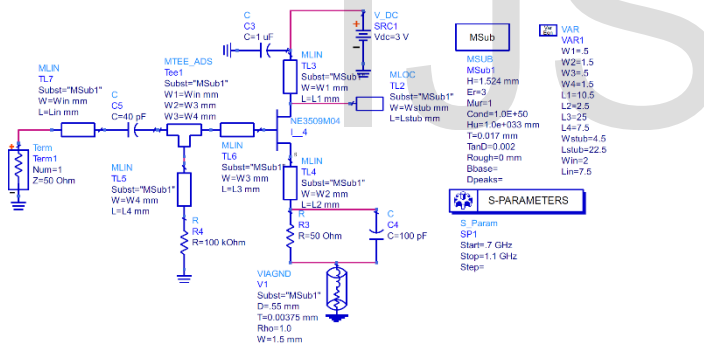


Figure 7: (a) The active circuit with negative input impedance. (b) The simulated input impedance of the active circuit and the antenna.

than one means the real part of the input impedance is

negative.

These instability criteria are at the outside of the stability circles for stable amplifier design which have been discussed in [32].

We have used a HJ GaAs FET transistor from NEC with 3509M04 part number as a super low noise figure transistor. The stability factor K of 3509M04 is checked and  $K < 1$ , which means the transistor is potentially unstable. There are some values for the load termination which make  $\Gamma_{in} > 1$ .

Figures 7a show the schematic of the active negative resistance circuit and the proposed antenna simulated in ADS, respectively. In order to set the DC bias point of a FET transistor, the gate voltage must be negative with respect to the source voltage ( $V_{GS} < 1$ ). This condition can be obtained by using a resistor in the source in DC mode and bypass it with a large capacitor in AC mode. In addition, the gate is connected to the ground with a high impedance resistor [32]. The input impedance of the active circuit and the miniaturized antenna are illustrated in Fig. 7b.

As can be seen in Fig.7c, the input impedance of the antenna

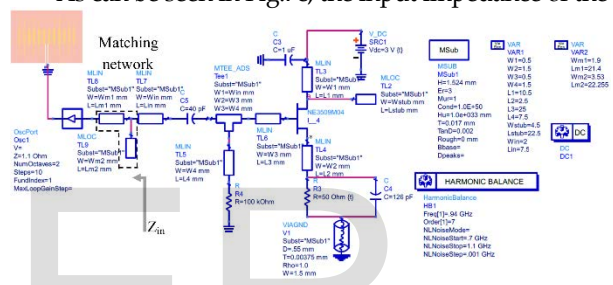


Figure 8: The circuit block diagram of the proposed AIA.

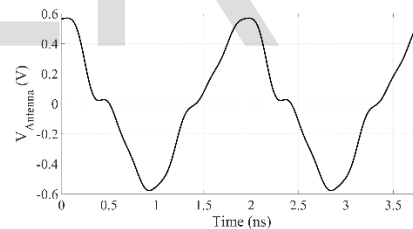


Figure 9: The output oscillation voltage of the AIA.

is  $Z_{in}^{Antenna} = 26 + j25.5$  and the input impedance of the active circuit is  $Z_{in}^{NRC} = -14 + j1.5$ . From Eq. (3), the sum of the input impedance of the antenna and circuit must be zero for the steady state oscillation condition.

In [30] it is shown that a high rate of success up condition for starting up the oscillation is as following:

$$X_{in}^{Antenna} + X_{in}^{NRC} = 0, R_{in}^{Antenna} = |R_{in}^{NRC}|/3 \quad (6)$$

Where  $X_{in}$  and  $R_{in}$  represent the input reactance and resistance. Figure 8 shows the proposed active integrated antenna block diagram simulated in ADS. The input impedance of the antenna is matched to the start-up oscillation condition by using a matching network which is shown in this figure. Thus,  $Z_{in}$  satisfies the steady state oscillation. The output voltage of the active integrated antenna is calculated by harmonic balance simulator by ADS. The output wave form is shown in Fig. 9.

The proposed AIA with miniaturized antenna is oscillating now in 930 MHz which can be used as RF beacon or wireless power transmission. By using adjustable oscillator with tunable antenna such as proposed in [33], a reconfigurable AIA is achievable.

#### 4 CONCLUSION

An active integrated antenna with miniaturized microstrip patch antenna and active oscillator circuit has been presented in this article. The ESRR have been used to change the constitutive parameter of a dielectric substrate. As a results, the loaded dielectric substrate is a magneto-dielectric structure. The antenna on the proposed magneto-dielectric substrate has been miniaturized up to 70 % compare with a patch antenna on the unloaded dielectric substrate.

This miniaturized antenna has been used as the radiator in an AIA system. The AIA system has been realized by using a transistor base circuit to provide negative input resistance. The low profile proposed AIA can be used in wireless power transmission system or wireless identification applications in UHF band.

#### REFERENCES

- [1] J. Garnica, R. A. Chinga, and J. Lin, "Wireless power transmission: From far field to near field," *Proc. IEEE*, vol. 101, no. 6, pp. 1321-1331, June 2013.
- [2] S. Kim, A. Georgiadis, A. Collado, and M. M. Tentzeris, "An inkjet-printed solar-powered wireless beacon on paper for identification and wireless power transmission applications," *IEEE Trans. Microw. Theory Tech.*, vol. 60, no. 12, pp. 4178-4186, Dec 2012.
- [3] R. A. Flynt, L. Fan, J. A. Navarro, and K. Chang, "Low cost and compact active integrated antenna transceiver for system applications," *IEEE Trans. Microw. Theory Tech.*, vol. 44, no. 10, pp. 1642-1649, Oct 1996.
- [4] C. M. Montiel, L. Fan, and K. Chang, "A novel active antenna with self-mixing and wideband varactor-tuning capabilities for communication and vehicle identification applications," *IEEE Trans. Microw. Theory Tech.*, vol. 44, no. 12, pp. 2421-2430, Dec 1996.
- [5] R. Marante, N. Ruiz, J. A. Garc a, and L. Cabria, "An EER based phase conjugator for retrodirective response using modern wireless signal formats," in 2012 6th European Conference on Antennas and Propagation (EUCAP), March 2012, pp. 3078-3081.
- [6] Z. H. Liu, Y. W. Chang, and T. G. Ma, "High-efficiency self-oscillating active integrated antenna using metamaterial resonators and its application to multicarrier radio frequency identification systems," *IEEE Trans. Antennas Propag.*, vol. 64, no. 9, pp. 3803-3810, Sept 2016.
- [7] D. D. Arumugam, M. Sibley, J. D. Griffin, D. D. Stancil, and D. S. Ricketts, "An active position sensing tag for sports visualization in american football," in RFID (RFID), 2013 IEEE International Conference on, April 2013, pp. 96-103.
- [8] S. Caizzone and E. DiGiampaolo, "Wireless Passive RFID Crack Width Sensor for Structural Health Monitoring," *IEEE Sens. J.*, vol. 15, no. 12, pp. 6767-6774, Dec 2015.
- [9] T. Negishi, F. Farzami, V. Picco, D. Erricolo, G. Gennarelli, F. Soldovieri, L. L. Monte, M. C. Wicks, and F. Ansari, "Detection and imaging of cracks in reinforced concrete structures using rf tomography: Quadratic forward model approach," in 2015 IEEE International Geoscience and Remote Sensing Symposium (IGARSS), July 2015, pp. 3552-3555.
- [10] R. Y. Miyamoto, K. M. K. H. Leong, S.-S. Jeon, Y. Wang, Y. Qian, and T. Itoh, "Digital wireless sensor server using an adaptive smart-antenna/retrodirective array," *IEEE Trans. Veh. Technol.*, vol. 52, no. 5, pp. 1181-1188, Sept 2003.
- [11] C. M. Montiel, L. Fan, and K. Chang, "An X-band self-mixing oscillator antenna for transceiver and spatial power-combining applications," *IEEE Trans. Microw. Theory Tech.*, vol. 46, no. 10, pp. 1546-1551, Oct 1998.
- [12] O. Manoochehri, S. Abbasniazare, A. Torabi, and K. Forooraghi, "A Second-Order BPF Using a Miniaturized-Element Frequency Selective Surface," *Progress In Electromagnetics Research C*, vol. 31, pp. 229-240, 2012.
- [13] M. Noroozariab, Z. Atlasbaf, and F. Farzami, "Substrate integrated waveguide loaded by 3-dimensional embedded split ring resonators," *AEU-Int. J. Electron. Commun.*, vol. 68, no. 7, pp. 658 - 660, 2014.
- [14] J. Wang, S. Qu, Z. Xu, H. Ma, Y. Yang, and C. Gu, "A controllable magnetic metamaterial: Split-ring resonator with rotated inner ring," *IEEE Trans. Antennas Propag.*, vol. 56, no. 7, pp. 2018-2022, July 2008.
- [15] M. Noroozariab, Z. Atlasbaf, M. Rafaei-Booket, and F. Farzami, "A tunable transmission line based on a SIW loaded by a new single-cell metamaterial," in Telecommunications (IST), 2012 Sixth International Symposium on, Nov 2012, pp. 75-79.
- [16] M. A. Salari, O. Manoochehri, and S. Abbasniazare, "Miniaturized microstrip ring hybrid with defected microstrip structure," *Microw. Opt. Technol. Lett.*, vol. 55, no. 10, pp. 2245-2248, 2013.
- [17] S. Abbasniazare, K. Forooraghi, A. Torabi, and O. Manoochehri, "Mutual coupling compensation for a 1x2 short helical antenna array using split-ring resonators," *Electromagnetics*, vol. 33, no. 1, pp. 1-9, 2013.
- [18] M. A. Salari, S. Abbasniazare, and O. Manoochehri, "The effect of electromagnetic waves on multilayer orthogonal microstrip lines with and without defected microstrip structure," *IEEE Antennas Wirel. Propag. Lett.*, vol. 11, pp. 1206-1209, 2012.
- [19] H. Mosallaei and K. Sarabandi, "Design and modeling of patch antenna printed on magneto-dielectric embedded-circuit metasubstrate," *IEEE Trans. Antennas Propag.*, vol. 55, no. 1, pp. 45-52, Jan 2007.
- [20] P. M. T. Ikonen, K. N. Rozanov, A. V. Osipov, P. Alitalo, and S. A. Tretyakov, "Magneto-dielectric substrates in antenna miniaturization: Potential and limitations," *IEEE Trans. Antennas Propag.*, vol. 54, no. 11, pp. 3391-3399, Nov 2006.
- [21] F. Farzami, K. Forooraghi, and M. Noroozariab, "Miniaturization of a microstrip antenna using a compact and thin magneto-dielectric substrate," *IEEE Antennas Wirel. Propag. Lett.*, vol. 10, pp. 1540-1542, 2011.
- [22] F. Farzami, K. Forooraghi, and M. Noroozariab, "Design and Modeling of a Miniaturized Substrate Integrated Waveguide Using Embedded SRRs," *IEEE Antennas Wirel. Propag. Lett.*, vol. 10, pp. 713-716, 2011.
- [23] F. Farzami and M. Noroozariab, "Experimental Realization of Tunable Transmission Lines Based on Single-Layer SIWs Loaded by Embedded SRRs," *IEEE Trans. Microw. Theory Tech.*, vol. 61, no. 8, pp. 2848-2857, Aug 2013.
- [24] C. H. Wu and T. G. Ma, "Miniaturized self-oscillating active integrated antenna with quasi-isotropic radiation," *IEEE Trans. Antennas Propag.*, vol. 62, no. 2, pp. 933-936, Feb 2014.
- [25] Y. Y. Lin, C. H. Wu, and T. G. Ma, "Miniaturized self-oscillating annular ring active integrated antennas," *IEEE Trans. Antennas Propag.*, vol. 59, no. 10, pp. 3597-3606, Oct 2011.
- [26] C. A. Balanis, *Modern antenna handbook. plus 0.5em minus 0.4em* John Wiley & Sons, 2011.
- [27] J. B. Pendry, A. J. Holden, D. Robbins, and W. Stewart, "Magnetism from conductors and enhanced nonlinear phenomena," *IEEE Trans. Microw. Theory Tech.*, vol. 47, no. 11, pp. 2075-2084, 1999.
- [28] D. Smith, D. Vier, T. Koschny, and C. Soukoulis, "Electromagnetic parameter retrieval from inhomogeneous metamaterials," *Physical review E*, vol. 71, no. 3, p. 036617, 2005.

- [29] K.Liu, S.M. El-Ghazaly, M.R. Deshpande, V.Nair, N.El-Zein, and H.Goronkin, "Active antennas incorporating tunnel diodes-large signal model approach," IEEE Microw. Wirel. Compon. Lett., vol. 11, no. 8, pp. 331-333, Aug 2001.
- [30]G.Gonzalez, Foundations of oscillator circuit design. plus 0.5em minus 0.4emArtech House, 2007.
- [31] F. Amato, C. W. Peterson, B. P. Degnan, and G. D. Durgin, "A 45 $\mu$  W bias power, 34 dB gain reflection amplifier exploiting the tunneling effect for RFID applications," in 2015 IEEE International Conference on RFID (RFID), April 2015, pp. 137-144.
- [32] R. E. Collin, Foundations for microwave engineering. plus 0.5em minus 0.4emJohn Wiley & Sons, 2007.
- [33] S. Abbasniazare, O. Manoochehri, and K. Forooraghi, "A reconfigurable printed dipole antenna using RF PIN diodes," Microwave and Optical Technology Letters, vol. 56, pp. 1151-1155, 2014.

IJSER